# Comparative spectroscopic and electrochemical study of nitroindazoles: 3-Alcoxy, 3-hydroxy and 3-oxo derivatives

Jorge Rodríguez [a,b], Claudio Olea-Azar [a,*], German Barriga [a], Christian Folch [a], Alejandra Gerpe [c], Hugo Cerecetto [c], Mercedes González [c]

[a] *Departamento de Química Inorgánica y Analítica, Facultad de Ciencias Químicas y Farmacéuticas, Universidad de Chile, Chile*

[b] *Departamento de Química, Facultad de Ciencias Básicas, Universidad Metropolitana de Ciencias de la Educación, Chile*

[c] *Laboratorio de Química Orgánica, Facultad de Química-Facultad de Ciencias, Universidad de la República, Uruguay*

**Abstract**

Cyclic voltammetry and electron spin resonance techniques were used in the investigation of novel 3-alkoxy- and 3-hydroxy-1-[ω-(dialkylamino)alkyl]-5-nitroindazole derivatives. A self-protonation process involving the protonation of the nitro group was observed. The reactivity of the nitro-anion radical for these derivatives with glutathione, a biological relevant thiol, was also studied by cyclic voltammetry. These studies demonstrated that glutathione could react with radical species from 5-nitroindazole system. Also we demonstrated that nitro-anion radicals show three different patterns of delocalization where the indazole 1-lateral chain does not have major influence.

*Keywords:* 5-Nitroindazole; Cyclic voltammetry; ESR; *Trypanosoma cruzi*

## 1. Introduction

American Trypanosomiasis, or Chagas' disease, is one of the most relevant endemic trypanosomiasis in Central and South America. Chagas' disease is caused by the protozoa *Trypanosoma cruzi* (*T. cruzi*). Latest data from WHO indicates that over 24 million of people, 8% of Latin-American population, are infected or are serologically positive for *T. cruzi*. Medication for Chagas' disease is usually effective when it is given during the acute stage of infection. No medication has been proven to be effective once the disease has progressed to later stages. Moreover, this pathology is treated with synthetic drugs such as Nifurtimox® (Nfx) and Benznidazole®, two nitro-containing heterocycles. The chemotherapy is still inadequate due to its undesirable side effects, including cardiac and/or renal toxicity. This explains the constant need for discovering and to investigate new effective chemotherapeutic and chemoprophylactic agents against *T. cruzi* [1,2]. In this sense, we have synthesized a series of indazoles as potential anti-*T. cruzi* agents [3–5]. In these studies, the 5-nitroindazole derivatives were identified as good in vitro antiparasites, being compound **1** (Scheme 1) the most selective trypanosome/mammal agent. Recently, efforts directed to obtain a novel series of 3-alkoxy or 3-hydroxy-1-[ω-(dialkylamino)alkyl]-5-nitroindazole and evaluate its antiprotozoa properties have been performed. Two groups of compounds have been prepared (5-NI, Scheme 1), the 3-alkoxy- and 3-hydroxy-1-[ω-(dialkylamino)alkyl]-5-nitroindazoles, series A, and the corresponding indazole[1,2-*a*]1,2-diazepines, series B [6].

Little information has been gathered related to the mechanism of action of these compounds. However, the reduction of the nitro group may be a key step in its biological activitiy, as is observed for other nitro-heterocyclic systems. In this paper the family of the 5-NI indazole derivatives was electrochemically studied in aprotic solvent using cyclic voltammetry (CV) technique. The nitro-anion radical species were characterized using

* Corresponding author. Tel.: +56 2 9782834; fax: +56 2 7370567.
*E-mail address:* colea@uchile.cl (C. Olea-Azar).

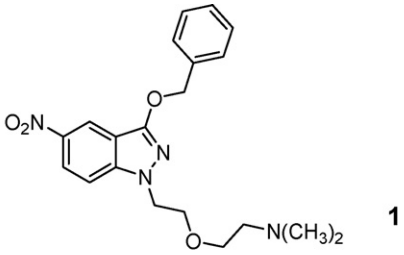

1

*New series of derivatives*

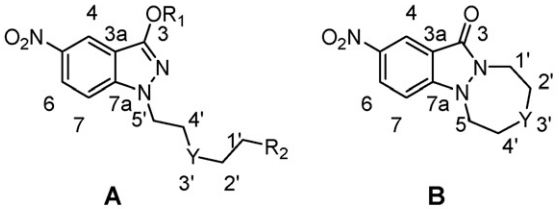

A B

| 5-NI | Structure | -$R_1$ | -$R_2$ | -Y- |
|---|---|---|---|---|
| **JNI 1** | **A** | -H |  | -O- |
| **JNI 2** | **B** | - | - | -O- |
| **JNI 3** | **B** | - | - | $-CH_2-$ |
| **JNI 4** | **A** | -Me | $-NH(CH_2)_3CH_3$ | $-CH_2-$ |
| **JNI 5** | **A** | -Bn | $-NH(CH_2)_3CH_3$ | $-CH_2-$ |
| **JNI 6** | **A** | -Bn |  | -O- |

Scheme 1. Chemical structure of 5-nitroindazole derivatives.

electron spin resonance spectroscopy (ESR). Also, we examined the interaction between the radical species generated from 5-NI and glutathione (GSH).

## 2. Materials and methods

### 2.1. Samples

The 5-NI derivatives (Scheme 1) were synthesized according to methods optimized in our previous works [5,6].

### 2.2. Cyclic voltammetry

Dimethylsulfoxide (DMSO) (spectroscopy grade) was obtained from Aldrich. Tetrabutylammonium perchlorate (TBAP), used as supporting electrolyte, was obtained from Fluka. CV was carried out using a Metrohm 693VA instrument with a 694VA Stand convertor and a 693VA Processor, in DMSO (ca. $1.0 \times 10^{-3}$ mol $L^{-1}$), under a nitrogen atmosphere at room temperature, with TBAP (ca. 0.1 mol $L^{-1}$), using a three-electrode cell. A hanging mercury drop electrode was used as the working electrode, a platinum wire as the auxiliary electrode and saturated calomel as the reference electrode.

### 2.3. ESR spectroscopy

ESR spectra were recorded in the X band (9.7 GHz) using a Bruker ECS 106 spectrometer with a rectangular cavity and 50 kHz field modulation. The hyperfine splitting constants were estimated to be accurate within 0.05 G. The anion radicals were generated by electrolytic reduction in situ using DMSO as solvent and TBAP as supporting electrolyte. All experiments were carried out at room temperature and under nitrogen atmosphere. The ESR spectra were simulated using the program WINEPR Simphonia 1.25 version.

### 2.4. Theoretical calculations

Density functional theory as implemented in the Spartan 04 [7] computational package was used to calculated and display spin density maps. The compounds were built with standard bond lengths and angles implemented in the program and the

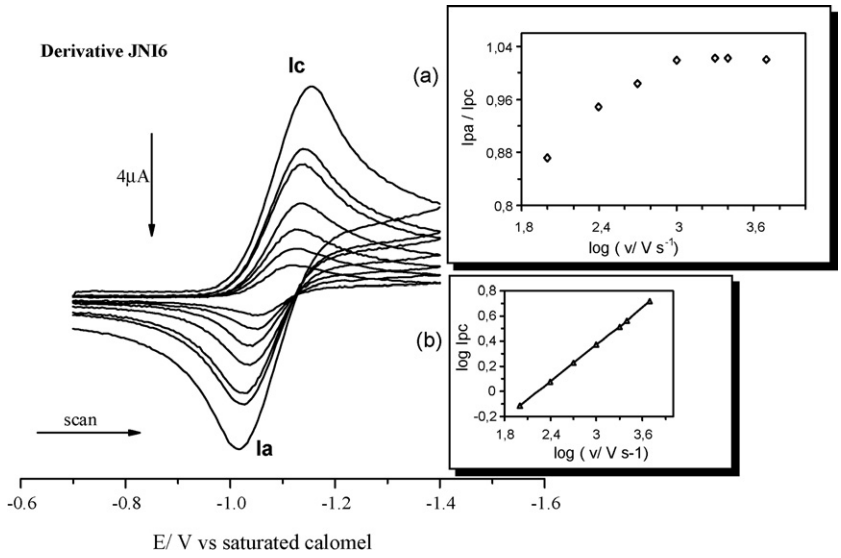


Fig. 1. Cyclic voltammograms of the isolated $RNO_2/RNO_2^{\bullet -}$ couple of **JNI 6** (1 mM) derivative in aprotic medium (DMSO + 0.1 M TBAP) and at different sweep rates (between 5000 and 100 mV $s^{-1}$). Insets: (a) current ratio vs. log(sweep rate); (b) cathodic peak current vs. log(sweep rate).

geometry of each molecule was fully optimized by applying semiempirical AM1 method in gas phase from the most stable conformer obtained using molecular mechanics (MMFF) methods. Then single point calculation using density functional methodology (Becke's three parameter exact exchange functional, B3) [8] combined with gradient corrected correlation functional of Lee–Yang–Parr (LYP) [9] of DFT method (U)B3LYP/6–31G* and calculations of electronic properties at (U)B3LYP/6–31G* [10,11].

## 3. Results and discussion

### 3.1. Cyclic voltammetry

In order to achieve the best experimental conditions that warranty the nitro-anion radical stability, an aprotic medium formed by DMSO and TBAP as supporting electrolyte was used. Under these conditions, all 5-NI derivatives displayed comparable voltammetric behaviour showing a very well-defined reversible reduction wave. Fig. 1 shows, as example, the voltammetric behaviour of **JNI 6** derivative. It can be observed that 5-NI derivatives **JNI 2–6** showed a one electron reversible transference process (peak Ic/Ia, around −1.0 V, Fig. 1) corresponding to the generation of the nitro-anion radical $RNO_2^{\bullet -}$. In addition, for derivatives **JNI 4** and **JNI 5** the $NO_2^{\bullet -}$-self-protonation phenomenon was not observed which indicate that N–H of the amino moiety, in $R_2$ substituent, is unable to protonate the free radical under the experimental conditions used. From the study of the dependence of the cathodic peak current, Ipc, with the sweep rate we have obtained a linear dependence with a slope of 0.487 (inset (b), Fig. 1) showing that the one electron reversible transference corresponds to diffusion controlled process without adsorption interference. In addition, the current ratio, Ipa/Ipc, increase when the sweep rate increase up to 1.0 (inset (a), Fig. 1). This result could indicate a typical variation of an ECi mechanism [12], showing values lower than 1.0 at low sweep rates and values around 1.0 at higher sweep rates. In this sense, the electrochemically generated nitro-anion radical could undergo two different decay paths, disproportionation or dimerization [13]. Table 1 lists the values of voltammetric cathodic and anodic peaks for all the compounds studied. All derivatives exhibited more negative potential values than Nfx (−0.91 V [14]) indicating a lesser capacity to be reduced.

Fig. 2 shows the typical voltammogram of 3-hydroxy-5-nitroindazole derivative **JNI 1**. Two reduction waves appeared, one cathodic peaks Ic (around −1.1 V) corresponding to nitro-anion radical $RNO^{2\bullet -}$ and a new wave at higher cathodic potential peak (IIc/IIa, around −1.4 V) corresponding to the reduction of the anion $–ORNO_2$ specie generated through a self-protonation reactions (C1). This process corresponds to an acid–base equilibrium in aprotic media, a typical behaviour of self-protonation phenomenon displayed by nitro-compounds with acidic moieties in their structures [4,15–17]. It is probably that the higher negative potential (couple IIc/IIa) of the 3-hydroxylate derivative corresponds to a diminish capacity to accept electrons due to its negative charge:

$$HORNO_2 + e \rightarrow HORNO_2^{\bullet -} \quad \text{(E 1)}$$

$$HORNO_2^{\bullet -} + HORNO_2 \rightarrow HORNO_2^{\bullet}H + {}^{-}ORNO_2 \quad \text{(C 1)}$$

$${}^{-}ORNO_2 + e \rightarrow {}^{-}ORNO_2^{\bullet -} \quad \text{(E 2)}$$

Table 1
Characteristic CV parameters in DMSO vs. saturated calomel electrode (sweep rate 2 V $s^{-1}$)

| 5-NI | $E_{pc}$ (V) | $E_{pa}$ (V) | $\Delta E$ (V) | $E_{1/2}$ (V) | Ipa/Ipc |
|---|---|---|---|---|---|
| **JNI 1** | −1.36 | −1.24 | −0.12 | −1.30 | 1.04 |
| **JNI 2** | −1.13 | −1.00 | −0.13 | −1.06 | 1.00 |
| **JNI 3** | −1.10 | −1.00 | −0.10 | −1.05 | 1.02 |
| **JNI 4** | −1.12 | −1.00 | −0.12 | −1.06 | 1.03 |
| **JNI 5** | −1.13 | −1.03 | −0.10 | −1.08 | 1.02 |
| **JNI 6** | −1.14 | −1.03 | −0.11 | −1.08 | 1.01 |

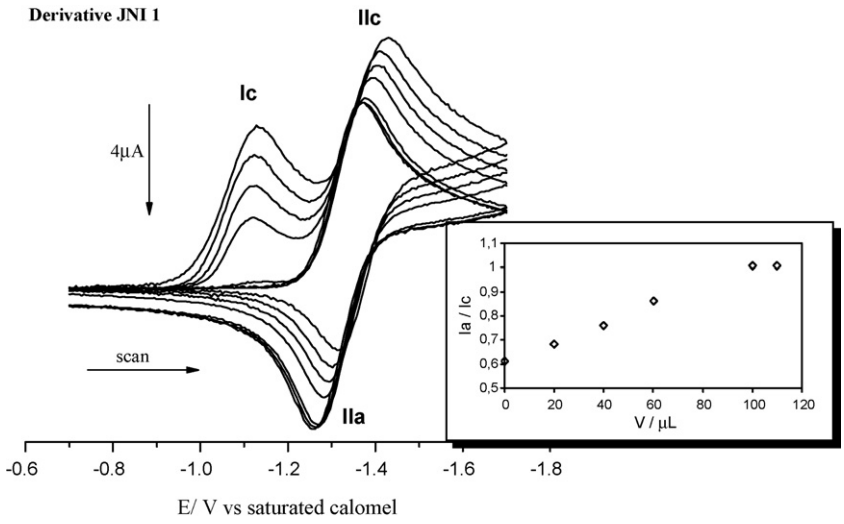


Fig. 2. CV of **JNI 1** derivative (1 mM) in DMSO (0.1 M TBAP) for different amounts of aqueous NaOH (0.1 M), sweep rates 1 V $s^{-1}$. Inset: current ratio (peak II) vs. the amount of NaOH (0.1 M) in µL.

In order to obtain suitable conditions for the nitro-anion radical from the 3-hydroxylate derivative and verify the self-protonation mechanism proposed, we have worked in presence of increasing amounts of aqueous NaOH (0.1 M). Fig. 2 shows the typical voltammograms obtained for 3-hydroxy-5-nitroindazole derivatives in the presence of different amounts of base. The electroreduction wave Ic gradually disappears with the increase of NaOH concentration when going from 0 to 1 mM (Fig. 2). The calculated Ipa/Ipc ratio using the Nicholson and Shain equation [18,19] increases to about 1.0 with the addition of NaOH for peak IIc/IIa in the case of 3-hydroxy-5-nitroindazole derivative (inset Fig. 2). We confirm the mechanism ECErev proposed for this 3-hydroxy-5-nitroindazole derivative given by the increment in the Ipa/Ipc ratio toward the reversibility of its final peak.

### *3.2. Reactivity of the nitro-anion radical anion electrochemically generated from 5-NI with GSH*

In order to study the capacity of nitro-anion radical of 5-NI to react with a natural antioxidant such as GSH, we studied by CV the effect of the GSH concentration on the Ipa/Ipc ratio or IIpa/IIpc ratio for the **JNI 6** derivative. The concentration of GSH was modified by adding increasing amounts of GSH (0.1 M in buffer phosphate pH 7.4) to the medium until the complete absence of the anodic peak. Fig. 3 shows the isolated couple of the typical 5NI CV in DMSO in the absence and in the presence of increasing amounts of GSH. This couple change when GSH was added, it can be observe that the cathodic peak increases significantly. In the case of 3-hydroxy-5-nitroindazole derivative, **JNI 1**, a large increase in the 1-electron $HORNO_2$ reduction step corresponding to the electroreduction of uncharged species (E 1) and the absence of the return oxidation step are observed when GSH was added to the medium. On the other hand, the other cathodic and anodic peaks disappeared (data not shown), which could indicate that the oxidation of GSH is faster than the proposed self-protonation mechanism. When the 3-hydroxy-5-nitroindazole derivative was previously treated with NaOH, the addition of GSH to the medium produces a large increase in the 1-electron $–ORNO_2$ reduction step corresponding to the electroreduction of charged species (E 2). The absence of the return oxidation step is also observed. This could indicate that the GSH reacts with both radical species ((E 1) and (E 2)). The GSH signals did not interfere with the corresponding nitro-anion radical detection at the studied concentrations [20–22]. These results indicated that the electrochemically obtained nitro-anion radical $RNO_2^{\bullet -}$ is immediately re-oxidized to the original material by the action of GSH. The effect is essentially catalytic, since the nitro-voltammetric changes were virtually complete. The species responsible for redox cycling were not identified, but it is possible that the $–S^{\bullet}$ radical (produced via the 1 electron oxidation of GSH) be the oxidizing agent for the $RNO_2^{-\bullet}$. The fact that in biological medium high thiol levels is present, this kind of process could take place in the parasite explain-

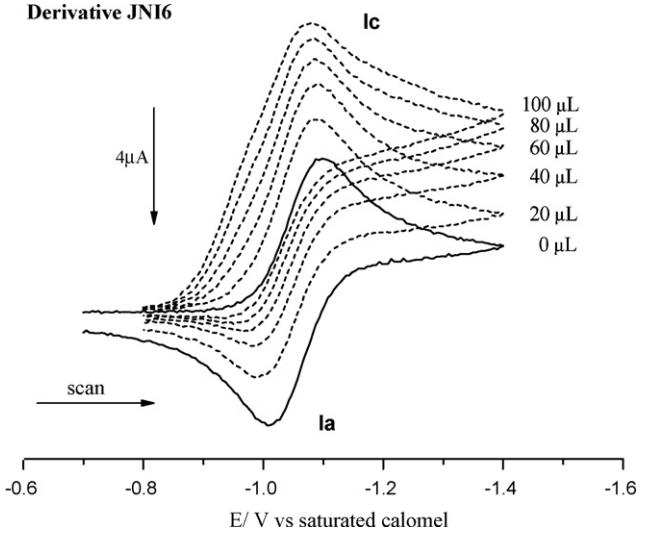


Fig. 3. CV of **JNI 6** (1 mM) in DMSO (0.1 M TBAP) for different amount of GSH (0.1 M in buffer phosphate pH 7.4), sweep rates 1 V $s^{-1}$.

Table 2
Hyperfine coupling constants and *g* value of the simulated 5-NI free radical spectrum

| 5-NI | $N_{NO_2}$ | N-1 | N-2 | H-4 | H-6 | H-7 | *g* value |
|---|---|---|---|---|---|---|---|
| **JNI 1** | 12.324 | 0.210 | 0.210 | 4.178 | 2.047 | 1.671 | 2.017 |
| **JNI 3** | 10.540 | 1.180 | 0.200 | 4.640 | 2.360 | 1.180 | 2.013 |
| **JNI 4** | 11.350 | 0.215 | 0.215 | 5.500 | 2.000 | 1.100 | 2.023 |

ing the observed biological activity for 5-NI derivatives against *T. cruzi*.

### 3.3. Electron spin resonance

5-NI free radicals characterized by ESR were prepared in situ by electrochemical reductions in DMSO by applying the potential corresponding to peak Ic or IIc obtained from the CV experiments. The interpretation of the ESR by means of a simulation process confirmed the stabilities of these radical species due to the delocalization of the unpaired electron. The simulation of the spectra was made by using hyperfine coupling constants (hfccs) obtained experimentally, modifying the line width, modulation amplitude and Lorentzian/Gaussian component until the resulting spectra reached the greatest similarity with the experimental ones. Table 2 presents the hfccs obtained for **JNI 1**,

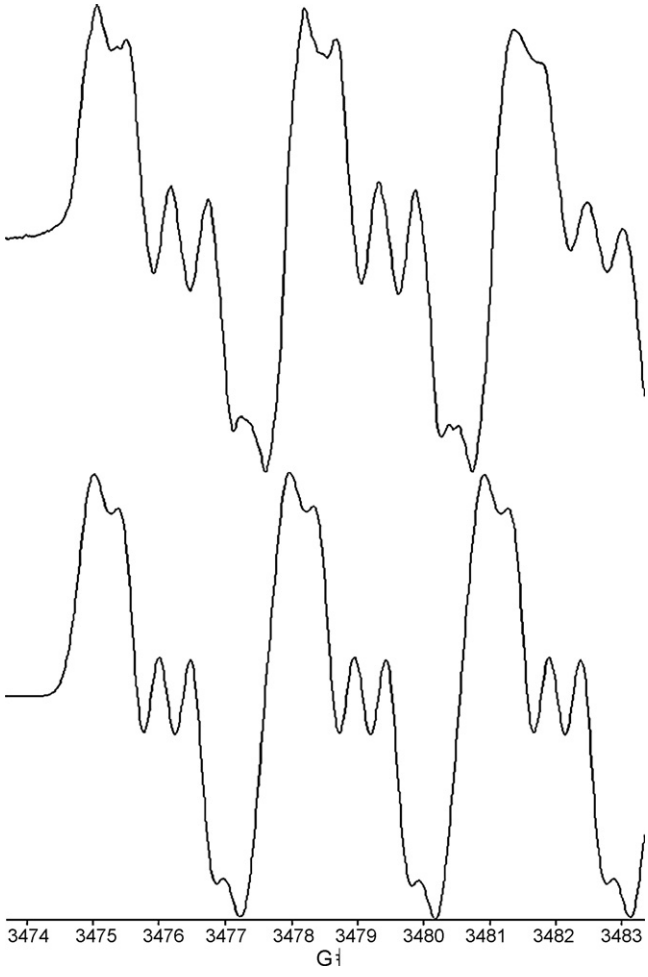


Fig. 4. ESR experimental spectrum of the dianion radical of compound JNI 1 in DMSO and computer simulation of the same spectrum. Spectrometer conditions: microwave frequency, 9.72 GHz; microwave power, 20 mW; modulation amplitude, 0.98 G; receiver gain, 59 db. Spectrum was simulated using the following parameters: line width = 1.87 G, Lorentzian/Gaussian ratio = 0.60 and the hyperfine constants are included in Table 2.

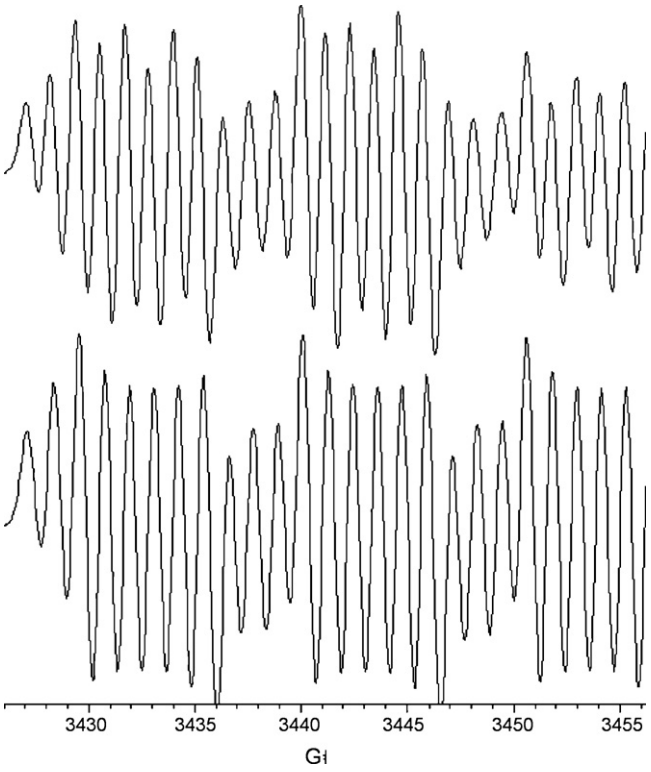


Fig. 5. ESR experimental spectrum of the anion radical of compound **JNI 2** in DMSO and computer simulation of the same spectrum. Spectrometer conditions: microwave frequency, 9.70 GHz; microwave power, 20 mW; modulation amplitude, 0.98 G; receiver gain, 30 db. Spectrum was simulated using the following parameters: line width = 0.3 G, Lorentzian/Gaussian ratio = 0.6001 and hyperfine constants are included in Table 2.

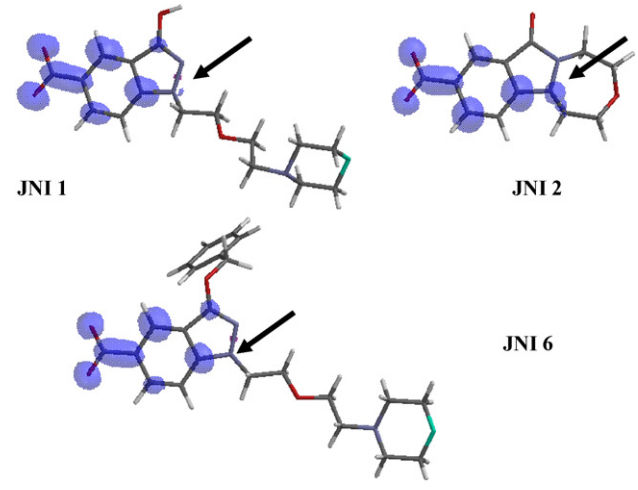


Fig. 6. Spin density surfaces (blue, isovalue 0.003, AM1/6–31G*) for compounds **JNI 1**, **JNI 2** and **JNI 6**. The arrows show N1-indazole atoms spin density. (For interpretation of the references to colour in this figure legend, the reader is referred to the web version of the article.)

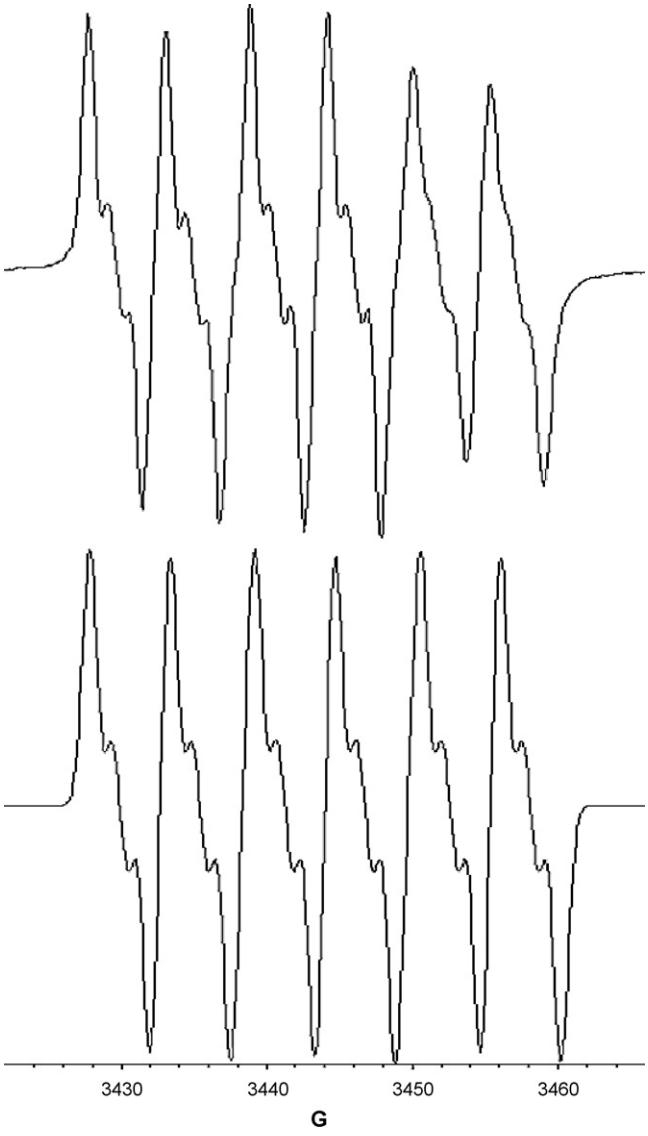


Fig. 7. ESR experimental spectrum of the anion radical of compound **JNI 6** in DMSO and computer simulation of the same spectrum. Spectrometer conditions: microwave frequency, 9.75 GHz; microwave power, 20 mW; modulation amplitude, 0.98 G; receiver gain, 30 db. Spectrum was simulated using the following parameters: line width = 0.95 G, Lorentzian/Gaussian ratio = 0.6 and hyperfine constants are included in Table 2.

**JNI 3** and **JNI 4** free radicals. The simulated spectrum of **JNI 1** radical (Fig. 4) corresponds to one triplet of nitrogen from nitro group and three doublets from H-4, H-6 and H-7. Fig. 5 displays a simulated spectrum for **JNI 2**, in terms of two triplets corresponding to the nitrogen atoms of the nitro group and the N1 indazole and three doublets assigned to nuclei H-4, H-6 and H-7. This hyperfine pattern shows that only one nitrogen of the indazole moiety is coupled with the free radical. This could indicate that the nitrogen N-1 shows a larger electronic density than the nitrogen N-2 adjacent to carbonyl group. The spin maps are completely in agreement with these results (Fig. 6). **JNI 4** free radical spectra was simulated in terms of one triplet assigned to nitro-nuclei N and three doublets assigned to nuclei H-4, H-6 and H-7 of the indazole moiety. Derivatives **JNI 4**, **5** and **6** showed the same pattern (Fig. 7). The hyperfine coupling constants (hfccs) obtained from three pattern observed in the ESR study of the family of the 5-NI are shown in Table 2.

## 4. Conclusion

Our CV results show that 3-alkoxy- or 3-hydroxy-1-[ω-(dialkylamino)alkyl]-5-nitroindazole derivatives are electrochemically reduced via formation of a nitro-anion radical. The reduction mechanism depends on the acidic moieties in their structures. A self-protonation process involving the protonation of the nitro group was also observed. The reduction mechanism proposed to 3-hydroxy-5-nitroindazole derivatives is an ECErev corresponding to the generation of the nitro-anion radical from uncharged species, followed by a self-protonation process from an hydroxyl moiety and the generation of a nitro-anion radical from negative charged species. On the other hand, GSH was capable of acting as an oxidizing agent for the 5-NI, regenerating the starting material from the nitro-anion radical. The oxidizing effect of GSH is supported by the parallel decrease of the anodic peak current and the increase of the cathodic peak in the CV, corresponding to the nitro-anion radical wave from uncharged species with the addition of GSH. Stable free radicals were generated using electrochemical reductions at potentials corresponding to the first wave and characterized by ESR spectroscopy. The 5-NI compounds studied showed three different patterns of spectrum depending on its structural characteristics. All these results indicated that the lateral chain does not have major influence on the electron delocalization. The ESR spectra pattern was similar for compounds **JNI 4** and **JNI 5** which correspond to 3-alkoxyindazole and 3-benzyloxyindazoles derivatives. In the case of compounds **JNI 2** and **JNI 3**, the different ESR pattern respect to the other 5-NI derivatives could be explained in terms of the molecular structure due to that they show a structure which facilitates the delocalization of the unpaired electron in the heterocyclic system. This is reflected in the major hyperfine coupling constant (hfccs) obtained for the nitrogen N1 of the indazole moiety (Table 2).

## Acknowledgments

This research was supported by FONDECYT 1071068 grant (Chile), MECESUP UMC-0204 grant (Chile), RTPD NETWORK, Comisión Sectorial de Investigación Científica–UdelaR CSIC 16/07-08 grant (Uruguay) and PEDECIBA (Uruguay).

## References

[1] S. Muelas, M. Suárez, R. Pérez, H. Rodríguez, C. Ochoa, J.A. Escario, A. Gómez-Barrio, Mem. Inst. Oswaldo Cruz 97 (2002) 269.
[2] H. Cerecetto, M. González, Curr. Top. Med. Chem. 2 (2002) 1185.
[3] A. Gerpe, G. Aguirre, L. Boiani, H. Cerecetto, M. González, C. Olea-Azar, C. Rigol, J.D. Maya, A. Morello, O.E. Piro, C. Ochoa, A. Azqueta, A. López de Ceráin, A. Monge, A. Rojas, G. Yaluff, Bioorg. Med. Chem. 14 (2006) 3467.
[4] C. Olea-Azar, H. Cerecetto, A. Gerpe, M. González, V.J. Arán, C. Rigol, L. Opazo, Spectrosc. Lett. 63 (2005) 36.

[5] V.J. Arán, C. Ochoa, L. Boiani, P. Buccino, H. Cerecetto, A. Gerpe, M. González, D. Montero, J.J. Nogal, A. Gómez-Barrio, A. Azqueta, A. López de Ceraín, O.E. Piro, E.E. Castellano, Bioorg. Med. Chem. 13 (2005) 3197.
[6] J. Rodríguez, A. Gerpe, G. Aguirre, O.E. Piro, C. Olea-Azar, M. González, H. Cerecetto, in preparation.
[7] Wavefunction Inc., 18401 Von Karman Avenue, Suite 370, Irvine, California 92612 USA.
[8] A.D. Becke, Phys. Rev. A 38 (1998) 3098.
[9] C. Lee, W. Yang, R.G. Parr, Phys. Rev. B 37 (1988) 785.
[10] M.J.S. Dewar, E.G. Zoebisch, E.F. Healy, J.J.P. Stewart, J. Am. Chem. Soc. 107 (1985) 3902.
[11] C.C.J. Roothaan, Rev. Mod. Phys. 23 (1951) 69.
[12] R.S. Nicholson, Anal. Chem. 36 (1964) 706.
[13] S. Bollo, L.J. Núñez-Vergara, J.A. Squella, J. Electroanal. Chem. 562 (2004) 9.
[14] C. Olea-Azar, A.M. Atria, F. Mendizábal, R. Di Maio, G. Seoane, H. Cerecetto, Spectrosc. Lett. 31 (1998) 99.
[15] J.A. Bautista-Martínez, I. González, M. Aguilar-Martínez, Electrochim. Acta 49 (2004) 3403.
[16] J. Carbajo, S. Bollo, L.J. Núñez-Vergara, A. Campero, J.A. Squella, J. Electroanal. Chem. 531 (2002) 187.
[17] G. Kokkinidis, A. Kelaidopoulou, J. Electroanal. Chem. 414 (1996) 197.
[18] R.S. Nicholson, Anal. Chem. 38 (1966) 1406.
[19] R.S. Nicholson, J. Shain, Anal. Chem. 36 (1964) 706.
[20] J.H. Tocher, D. Edwards, J. Biochem. Pharmacol. 50 (1995) 1367.
[21] L.J. Núñez-Vergara, J.A. Squella, C. Olea-Azar, S. Bollo, P.A. Navarrete-Encina, J.C. Sturm, Electrochim. Acta 45 (2000) 3555.
[22] R. Kizek, J. Vacek, L. Trnkova, J. Jelen, Bioelectrochemistry 63 (2004) 19.